DRAFT

Final Report for Project Entitled:

Full Scale Wind Load Testing of Aluminum Screen Enclosures
PO Number A95F33

Performance Period: 1/6/2014 – 6/30/2014

Submitted on

June 15, 2014

Presented to the

Florida Building Commission
State of Florida Department of Business and Professional Regulation

by

Sungmoon Jung, Ph.D., sjung@eng.fsu.edu, (850) 410-6386, Technical Lead
Forrest J. Masters, Ph.D., P.E., masters@ce.ufl.edu, (352) 392-9537 x 1505, Principal Investigator

Designated Project Leader: Forrest Masters

Engineering School for Sustainable Infrastructure & Environment

Table of Contents

1. Applicable Sections of the Code

- 1609.1.1, Florida Building Code—Building
- 2002.4, Florida Building Code—Building

2. Executive Summary

2.1. Description of Issues

The letter from Joe Belcher on behalf of the Aluminum Association of Florida (AAF) describes the project (see Appendix). FBC Staff requested that we provide third-party technical input, witness testing, and provide a final review of the report.

Dr. Sungmoon Jung, Assistant Professor of Civil and Environmental Engineering at Florida State University, provided primary consultation with support from UF. Dr. Jung was selected based on his research experience in this area. More information on this work may be found in Schellhammer and Jung (2012) and Lewis et al. (2013).

2.2. Recommendations for the Code

The wind loading applied during the full-scale tests did not exceed the design loading. In principle, no members should have failed. However, failures occurred at non-structural and structural members, especially screen attachments and posts due to unbalanced loading.

The failure of screen attachments and unbalanced loading has direct implications on the rule on removing the screen (Rule 61G20-1.002). If some screens are cut but not others, unbalanced loading may accelerate the failure of the post. Code changes should be considered to either require removal of all screens above the chair rail, or, devise a more secure fastening of screen attachments to prevent partial failure and unbalanced loading.

The tested specimens received very thorough inspection and quality control. However, it is well known that the real-world plan review and inspection may not reach such a level, and therefore, likely experience much more severe failure due to the hurricane. The code requirement on this issue would greatly reduce potential failure of screen enclosures due to the hurricane.

Finally, the tensile ultimate strength and tensile yield strength of the aluminum extrusions, based on the testing of coupons harvested from the specimens, were lower than the specified values. To ensure that the aluminum meets or exceeds the specified performance levels, the building code should require that material certification be submitted to the building official.

3. Selection of Testing Specimens

3.1. Overview

An oversight committee consisting of members of the Aluminum Association of Florida (AAF) and the Insurance Institute for Business & Home Safety (IBHS) was formed. FBC staff (Mo Modani) and Chair of the Structural TAC (Jim Schock) also participated.

During the first meeting (January 15, 2014), Dr. Masters discussed the scope of work, its relation to the entire scope of projects funded by the Florida Building Commission, and facilitated introductions among the group. Joe Belcher then led a discussion on the original proposed plan. Drs. Jung and Reinhold discussed prior research and the IBHS facility, respectively.

The group agreed on performing comparative experimental testing of two screen enclosure systems. The first system will be based on signed and sealed, site-specific plans. This “generic” system will be based

on conventional design practice, which represents the majority of designs outside of the HVHZ in Florida. The second system will be identical to the "generic" system except that the design will conform to requirements set forth in the *2010 AAF Guide to Aluminum Construction in High Wind Areas*.

3.2. Details of the Selection Process

AAF acquired 35 signed and sealed, site-specific plans from the St. Johns County Building Department and the City of Jacksonville. Design criteria were either 120 mph Exposure B, 130 mph Exposure C, or 120 mph Exposure C. Ten designs with a mansard roof with approximate dimensions of 24 ft X 40 ft X 9 ft and a 48 in rise in the roof were selected, de-identified, and forwarded to Dr. Jung (FSU) to review.

Dr. Jung selected one plan, independent of stakeholder inputs, using the approach explained in the following. The selected plan was the one showing average structural performance among the ten candidate plans. This specimen will be referred as "Generic specimen." Once the Generic specimen was selected, then the AAF designed a second specimen similar in shape and size following the AAF Guide (AAF 2010). This specimen will be referred as "AAF specimen."

3.2.1. Ranking Criteria

In order to rank the candidate designs in an objective manner, ranking criteria were developed. Failure of any member is likely to cause subsequent failures of other members, and eventually collapse the entire structure. Therefore, failure of any type of member was included in the criteria. For certain type of failure (ex: failure of beams), although the failure at certain location may be more detrimental to the structure than the failure at another location, the difference was not considered because the difference is likely to be small given little redundancy in screen enclosures. Ideally, failure of connections should also be considered. However, drawings often did not clearly show connection details so it was difficult to compare their performance objectively. Therefore, failure of connections was not included in the criteria. The developed criteria and rationale are shown below.

Since the time-frame of the project did not allow finite element analysis of individual candidate structures, the "Screen Enclosure Structural Calculator" (referred as the Tool) was utilized to obtain input to these criteria. The Tool provided approximate analysis results of screen enclosures given specimen dimensions and member properties. The Tool may have introduced small errors because of approximate nature of the analysis, but it was sufficient to rank candidates.

Failure of roof bracing and wall bracing (relative importance = 30%)

Among different types of members, higher weights were given to roof bracing and wall bracing because their failure is likely to lead to the collapse sooner than the failure of other types. When they are intact, they prevent rotation of beams due to the wind loading. When they fail, the beams rotate (assuming beam-to-host connections fail), which can cause catastrophic failure of the structure. The Tool provides two outputs on this category: "Diagonal Braces" (referred as B_1) and "Front Wall Bracing" (referred as B_2), each in percentage. 100% means the failure condition has reached. After converting the percentage to a number (100% = 1.0, 150% = 1.5, etc.), the following equation was used to calculate the damage contribution from the bracing.

$$D_{bracing} = (B_1 + B_2)/2 \times 0.3$$

in which $D_{bracing}$ is the damage contribution from the roof bracing and wall bracing. The factors were determined so that when both roof bracing and wall bracing reach 100% (= 1.0), the damage index becomes 0.3 or relative importance of this category. Higher failure probability will be penalized with a higher damage index.

Redundancy in roof bracing and wall bracing (relative importance = 40%)

Since the roof and wall bracings are critical in preventing enclosure performance, additional parameters were introduced to consider their redundancy. The parameter R_1 addresses the redundancy in the roof bracing. If roof bracing near the host structure continues to the other end (i.e., forms a load path), then R_1

= 0 or does not contribute to damage index. If the bracing forms the load path mostly but are missing between two purlins once, R_1 = 0.5. If the bracing is missing twice or more (i.e., load path unlikely), R_1 = 1. Since all designs were symmetric, one of the two sides of the bracing was considered to check this. The parameter R_2 deals with the redundancy in the cable bracing. R_2 = 0 if two or more cables present on one corner (therefore four or more cables total). R_2 = 1 if one or no cable.

$$D_{redundancy} = (R_1 + R_2)/2 \times 0.4$$

Failure of posts (relative importance = 15%)

Failure of posts is very likely to cause failure of adjacent members due to the combination of wind loading and gravity. The Tool provides "Corner Posts" (referred as P_1), "Front Posts" (referred as P_2), and "Side Posts" (referred as P_3). The following equation was used for the damage contribution from this category.

$$D_{posts} = (P_1 + P_2 + P_3)/3 \times 0.15$$

Failure of purlins, eave rails, and beams (relative importance = 15%)

The last member category includes beams, purlins, and eave rails. The Tool provides "Purlins" (referred as O_1), "Eave Rails" (referred as O_2), and "Beams" (referred as O_3). The following equation was used for the damage contribution from this category.

$$D_{others} = (O_1 + O_2 + O_3)/3 \times 0.15$$

3.2.2. Ranking Results

The ten candidate plans were ranked according to the criteria. The original design plans are not included in this report due to the copyright issues, but their performance indices are summarized below in Table 1. The top ranking plan has the highest damage index, i.e., it has the worst structural performance.

Table 1. Ranking of expected structural performance of candidate structures (ranking #1 corresponds to the expected worst performance)

Plan ID	B1	B2	R1	R2	P1	P2	P3	O1	O2	O3	Damage Index	Ranking
11303480	2.237	1.116	1	1	1.224	1.094	0.906	0.605	0.509	1.926	1.216	1
11308820	1.977	0.875	1	1	1.104	1.034	0.587	0.633	0.35	2.998	1.163	2
11305289	1.637	2.221	0.5	1	1.191	1.102	0.581	0.666	0.89	1.152	1.158	3
11307939	1.586	0.963	0.5	1	1.013	0.886	0.621	0.495	0.42	5.189	1.114	4
11308225	1.691	1.016	1	0	1.107	0.764	0.552	0.556	0.404	2.138	0.882	5
11309823	1.334	2.285	0	0	1.04	0.971	0.758	0.363	0.501	2.285	0.839	6
11303812	1.252	1.294	0	0	1.733	1.046	0.774	0.37	0.542	1.171	0.664	7
11308882	0.991	0.585	0.5	0	0.954	0.741	0.407	0.662	0.282	1.871	0.582	8
11303074	0.961	0.966	0	0	1.018	0.912	0.496	0.274	0.36	2.217	0.553	9
11309038	0.995	0.489	0	0	0.851	0.872	0.424	0.346	0.29	1.616	0.443	10

Design plans with medium performance were 8225 (ranking #5) and 9823 (ranking #6). The plan 8225 was ultimately chosen as the specimen for the experiment, because the bracing and cable scheme of the plan 8225 was more representative compared to the plan 9823. Due to the approximate nature of the ranking, other designs in the medium range were also qualitatively checked, to ensure that a good candidate for the experiment was not missed. The plan 5289 (ranking #3) had only one set of cable exhibiting high stress. The plan 7939 (ranking #4) had extreme beam overstress. The height of plan 3812 (ranking #7) was too high (12.5 feet) that it was an outlier among the ten designs. Therefore, it was confirmed that the plan 8225 (ranking #5), qualitatively, was also the most representative among the ten designs without having any major issue.

3.3. Selected Specimens

The drawings of AAF specimen are shown in the Appendix (section 11.2). Connection details of this specimen follow the AAF guide (AAF 2010). Overall dimensions of both specimens are 24 ft × 37.5 ft × 11.25 ft. The eave height is 8.25 ft. Major differences between the Generic and the AAF specimens are:

- Generic posts are 2X4 SMB and 2X5 SMB whereas AAF posts are all 2X4 SMB
- Generic eave rails are 2X2 whereas AAF eave rails are 2X3
- Generic beams are 2X6 SMB whereas AAF beams are 2X8 SMB
- Generic purlins are 2X2 whereas AAF purlins are 2X3
- Generic uses 7” super gutter whereas AAF uses 5” super gutter
- AAF specimen has additional roof bracing and backing plates at some purlins
- AAF specimen does not have cables on the side walls
- Some AAF purlins require backing plates (at bracing bays)

4. Preliminary Analysis of Specimens

4.1. Preliminary Finite Element Analysis

In order to assist the experimental set up, finite element analysis was conducted for both specimens using SAP2000 (CSI 2009). Figure 1 shows the developed finite element model. All boundaries have fixed translations and freed rotations. Moment end-releases are shown with green dots in the figure. In reality these connections would have some moment resistance, but they were modeled as hinges due to the unavailability of their moment resistance.

For the aluminum, elastic modulus = 10100 ksi and Poisson’s ratio = 0.33 were used. For the cable, elastic modulus = 16000 ksi and Poisson’s ratio = 0.3 were used without pre-stress. Two load cases from the Florida Building Code were used (FBC 2010). The first load case used pressure on the windward wall, leeward wall, and suction on the roof. The second load case used pressure on the front wall, and suction on the roof. Exposure B, 120 mph wind loading was multiplied by 0.6 (to ASD) and 0.88 (screen). Therefore, the pressures on windward, leeward, and the roof were 10.6 psf, 7.9 psf, and 3.2 psf, respectively.

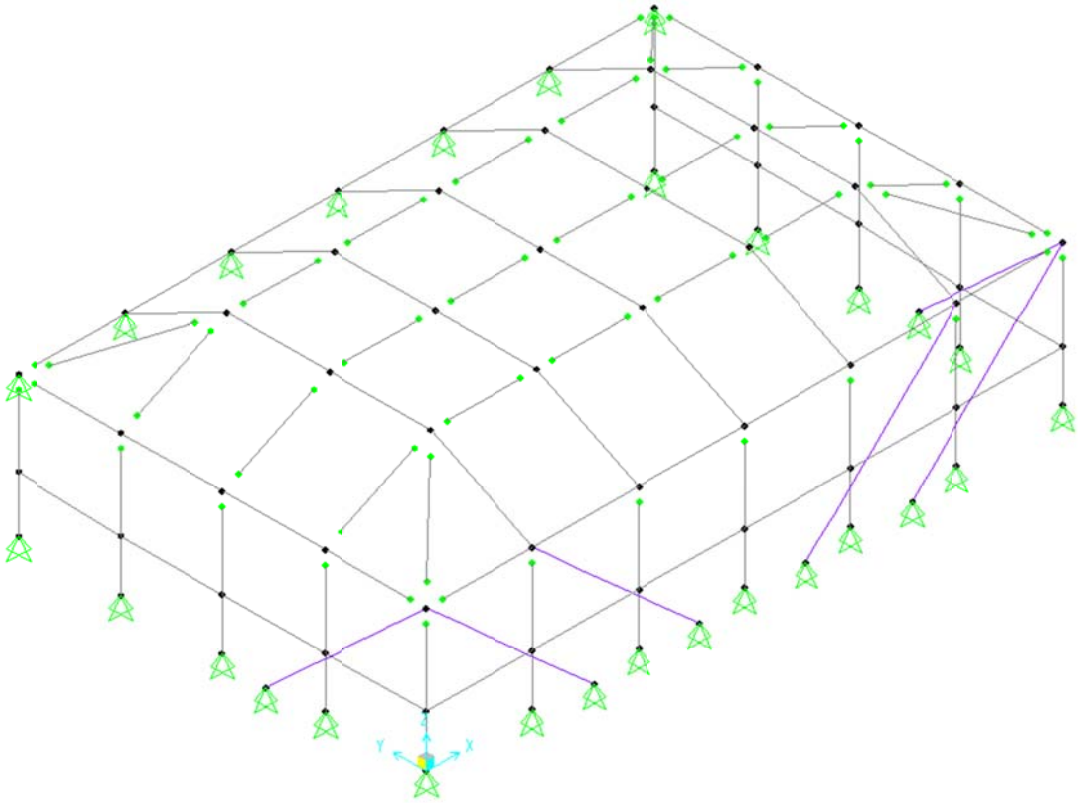

Figure 1. Finite element model of the Generic screen enclosure specimen (AAF specimen does not have side cables, but it has additional roof bracings)

4.2. Identification of Locations for Sensors

Moments and axial forces were obtained from the finite element analysis. Then, stress ratios were computed using (actual to allowable stress ratio: moment) = (finite element max moment) / (AAF 2010 Appendix A allowable moment) and (actual to allowable stress ratio: column) = (finite element max compressive force) / (ADM 2005 Table 2-20 based allowable compressive force). Members with high tensile forces were also identified.

In the figure, dotted lines represent the first load case whereas the solid lines represent the second load case. Red box means high actual to allowable stress ratio: moment (% is shown), green box means high actual to allowable stress ratio: column (% is shown), and blue box means high tension (kips is shown).

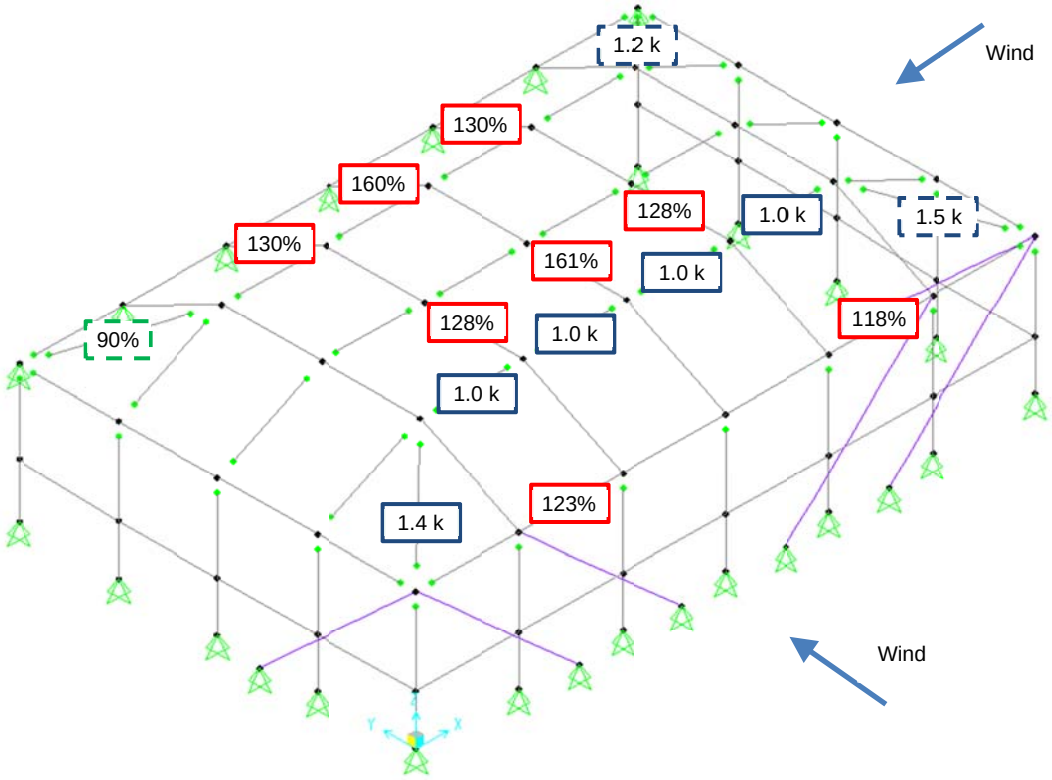

Figure 2. Members with high actual to allowable stress ratios and high tensile forces: Generic specimen

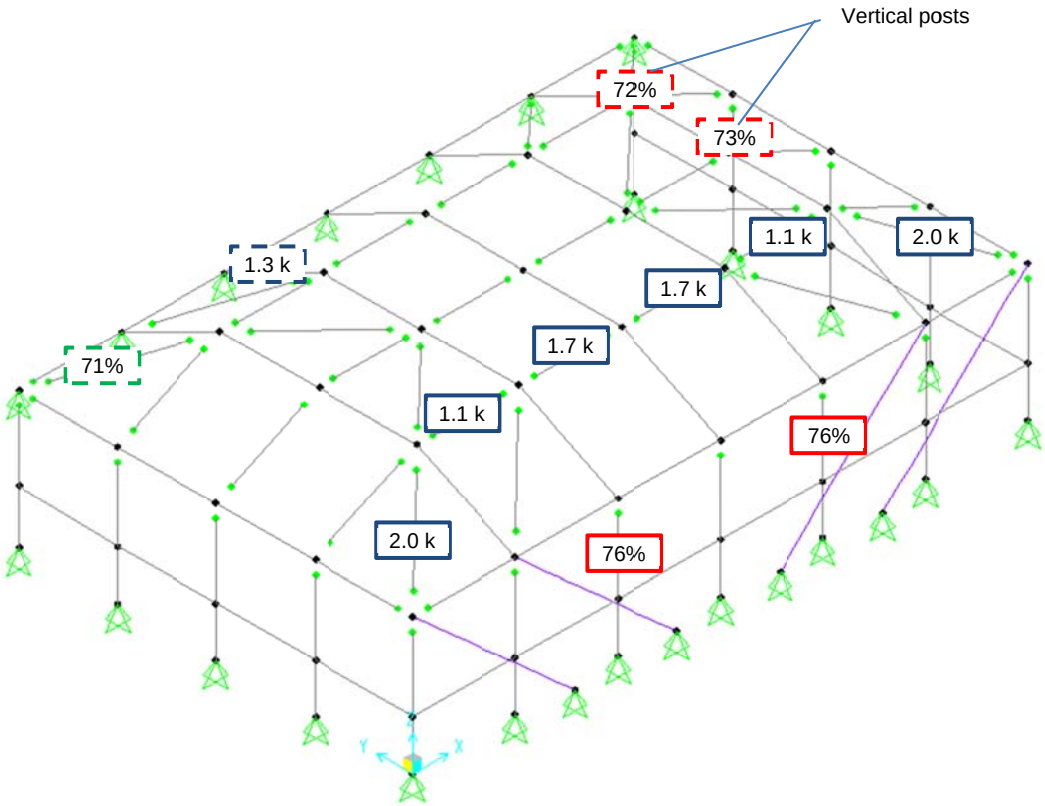

Figure 3. Members with high actual to allowable stress ratios and high tensile forces: AAF specimen

5. Experimental Set Up

5.1. Specimen Construction and Set Up

Experiments were conducted at the Insurance Institute for Business & Home Safety (IBHS) Research Center. The center has a state-of-the-art full-scale testing facility located in Richburg, South Carolina, that is capable of generating hurricane-strength winds. Materials for the specimens were fabricated in Florida and then transported to the center.

Both specimens were assembled at the IBHS Research Center. An 18 × 14 inch fiberglass mesh was used for both specimens. Figure 4 shows the Generic specimen in the testing chamber. The wind blows from the right to the left through the vanes. Figure 5 shows further details of the fans and the vanes. Both the host structure and the screen enclosure were built on top of I-beams that represent the foundation. This set up enabled the rotation of the entire specimen to study the effect of the changing the wind angle. Figure 6 shows how the specimen is connected to the host structure and the foundation. Figure 7 shows the AAF specimen in the testing chamber.

Figure 4. Generic specimen in the testing chamber

Figure 5. IBHS wind tunnel: fans and vanes

Figure 6. Specimen attachment to the host structure and the foundation

Figure 7. AAF specimen in the testing chamber

Cable tensions were applied after constructing the specimens. The installers were directed to tighten the cables as they would in the field. Cable tensions were measured using load cells. The cable tensions were then adjusted to achieve the average tension measured in the Generic specimen in order to have comparable cable tensions between the two specimens. For the Generic specimen (Figure 4), the final cable tensions were 188 lb, 183 lb, 187 lb, 190 lb, from left to right shown in the figure. For the AAF specimen (Figure 7), the final cable tensions were 186 lb, 179 lb, 191 lb, 186 lb, from left to right shown in the figure.

Figure 8. Load cell measuring the cable tension

5.2. Sensors

Multiple high-definition video cameras recorded the response of the specimen. To quantify the structural response, displacement, strain, and force were measured. The displacement sensor is OptiTrack Flex 3. The displacement sensors are shown in Figure 4 and Figure 7, on the I-beam outside of the screen enclosure.

A typical set up of strain gauges is shown in Figure 9. This set up is to measure the moment. Strain gauges are 0.25 inches from the edges of the beam. A close-up view of another strain gauge set up is shown in Figure 10. This set up measures both moment and axial force. The top and bottom gauges, also located on the opposite face, measure the moment whereas the center gauges measure the axial force (Hoffmann 1986).

Indices of all sensors are shown in Figure 11 for the generic specimen and Figure 12 for the AAF specimen. The locations were based on the preliminary analysis shown in section 4.2. Additional sensors were also installed to cover other members of interest. These indices will be used to report the results in later sections. The label prefix “A” represents axial force, “M” represents moment, and “C” represents cable tension.

Figure 9. Strain gauges installed in a beam to measure the moment

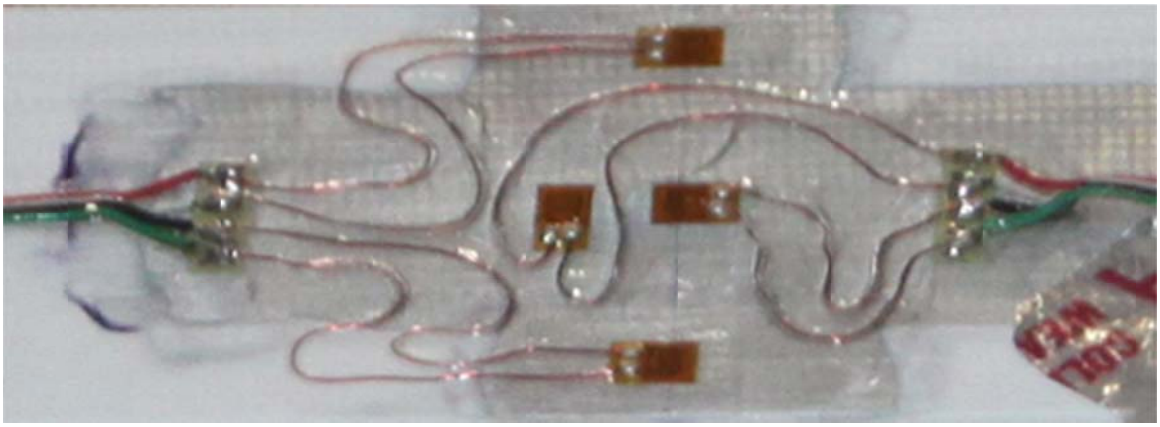

Figure 10. Strain gauges for both moment and the axial force

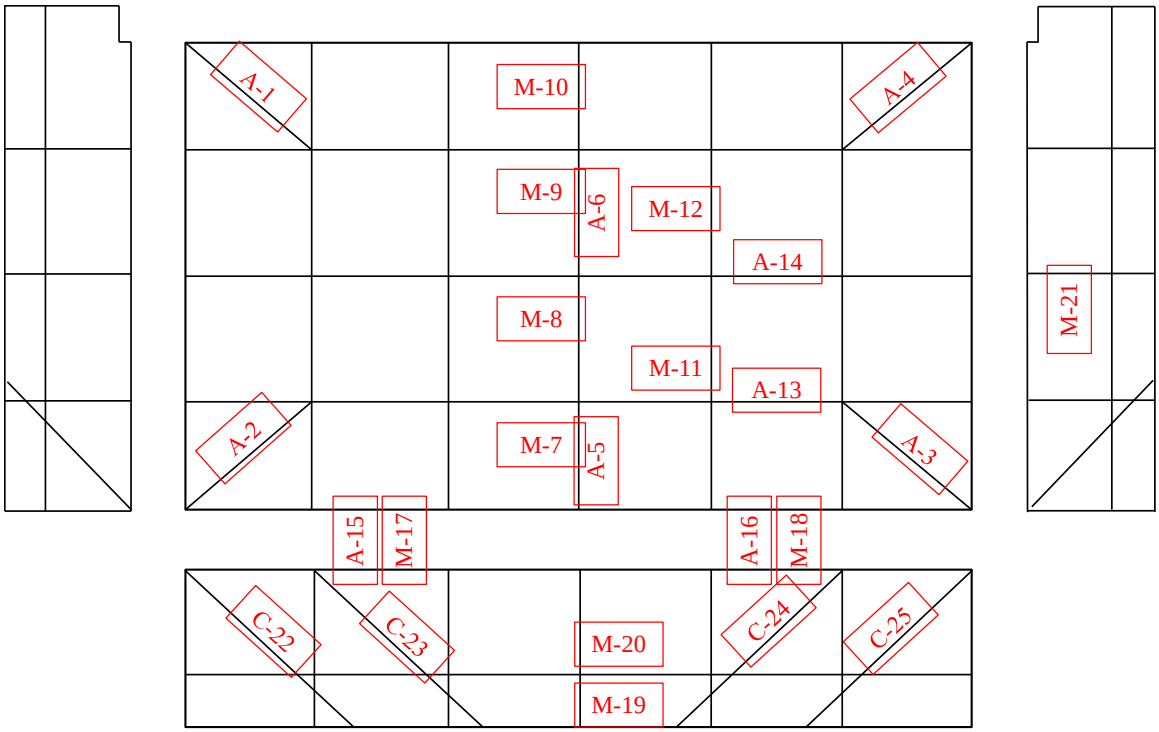

Figure 11. Sensor indices: generic specimen (A: axial, M: moment, C: cable)

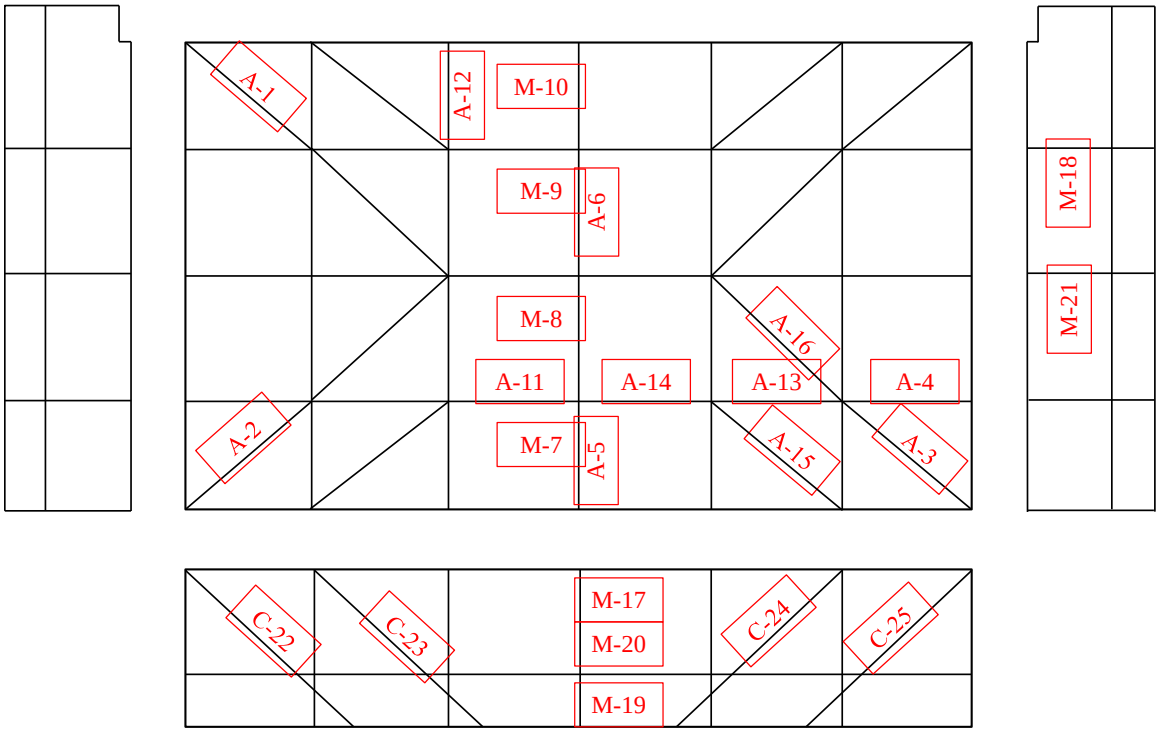

Figure 12. Sensor indices: AAF specimen (A: axial, M: moment, C: cable)

5.3. Static Pull Test Cases

Before conducting the wind load testing, static point loads were applied to the specimen while measuring the sensor responses. These tests are labeled as the static pull tests. The pull tests ensured that the

sensors functioned properly. Also, they provided data points useful for the calibration of analysis models.

Figure 13 shows the ten static pull test cases. The same patterns were used for both the generic and the AAF specimens. Each pull test case was composed of 4.75 lb, 29.65 lb, 53.8 lb, 78.45 lb, and 102.5 lb. Weight plates were added one at a time, and the vertical force was converted to the lateral force using a pulley mechanism shown in Figure 14.

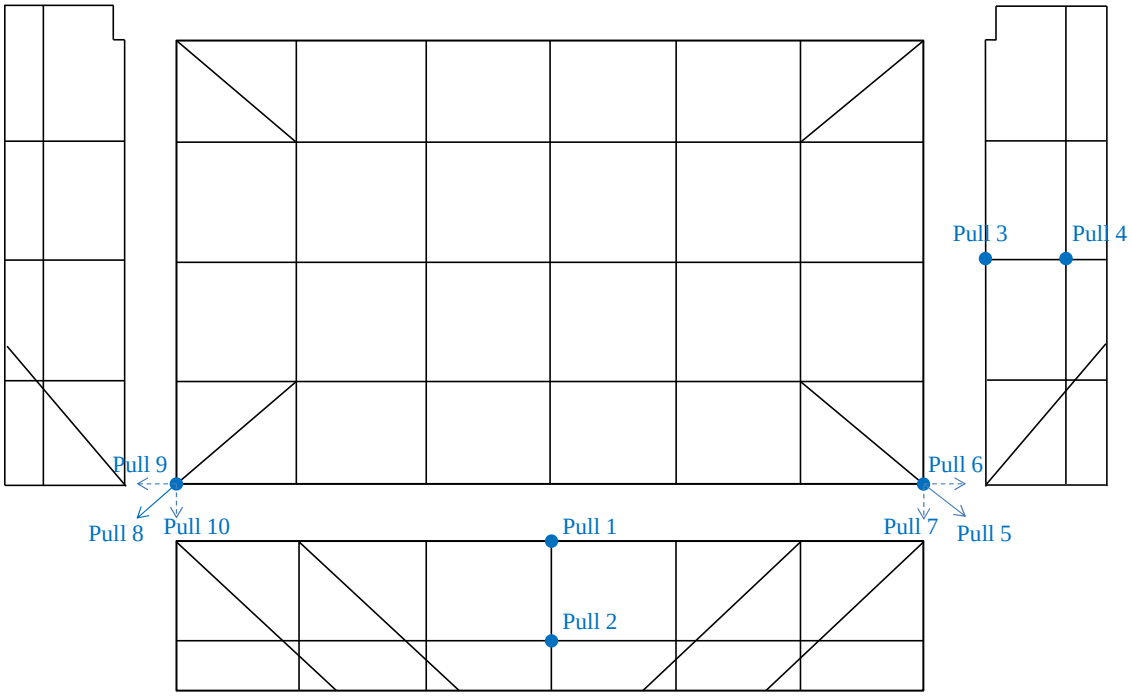

Figure 13. Static pull test cases for sensor testing and model calibration

Figure 14. The apparatus for applying the static point load

5.4. Wind Load Cases

The specimens were subjected to multiple wind load cases. Each load case had certain mean wind speed, wind angle, and turbulence characteristics. The 0 degree angle is when the wind blows on the front of the screen enclosure. The 90 degree angle is when the specimen is rotated 90 degrees clockwise from this 0 degree orientation. See Figure 15 for clarification.

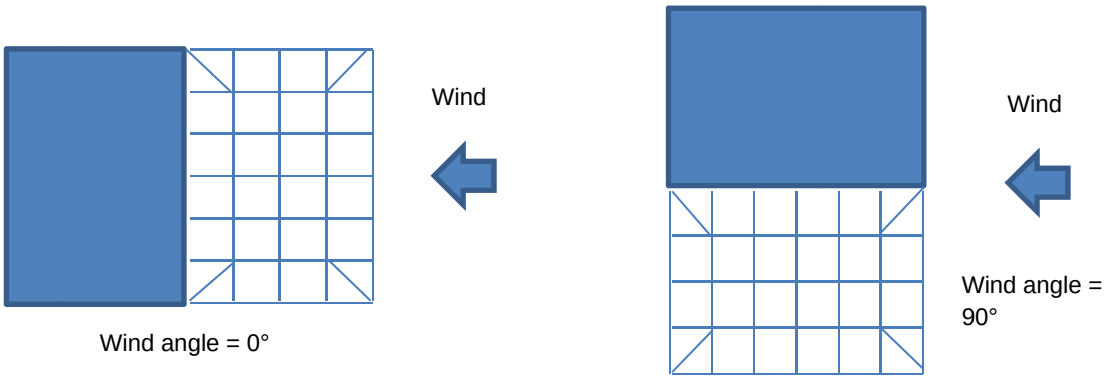

Figure 15. Definition of the wind angles

Four series of tests were performed. Series I evaluated the 90 degree case over three wind speed intensities with and without turbulence (Table 2). Series II repeated most of these tests across a range of wind angles (Table 3). Series III gradually increased the wind speed for 0 degree and 90 degree wind angles (Table 4). Series I through III were applied identically to both specimens.

Toward the end of the Series III, the two specimens responded differently. Therefore, the wind loading sequence had to be modified differently for the two specimens. This last part as termed as Series IV. The

wind loading sequence for the Generic specimen is shown in Table 5 whereas that for the AAF specimen is shown in Table 6. Unlike Series I through III, Series IV involved retrofitting part of the damaged screen and/or structure. Further details of the retrofit will be explained later when we discuss the experimental results.

The wind speed given in the table is at the standard height, i.e., 33 ft (10 m) from the ground.

Table 2. Wind loading series I: different speeds and turbulence (both specimens)

Runs	Angle (deg)	Maximum Wind Speed	Longitudinal Turbulence	Lateral Turbulence	Duration (minutes)
1	90	30	No	No	5
2	90	45	No	No	5
3	90	45	Yes*	Yes*	15
4	90	45	Yes	Yes	15
5	90	60	No	No	5
6	90	60	Yes	Yes	15

* Wind at each fan cell is identical, i.e. correlation = 1

Table 3. Wind loading series II: effect of wind angles (both specimens)

Runs	Angle (deg)	Maximum Wind Speed	Longitudinal Turbulence	Lateral Turbulence	Duration (minutes)
7	75	45	No	No	5
8	75	60	No	No	5
9	75	60	Yes	Yes	15
10	60	45	No	No	5
11	60	60	No	No	5
12	60	60	Yes	Yes	15
13	45	45	No	No	5
14	45	60	No	No	5
15	45	60	Yes	Yes	15
16	30	45	No	No	5
17	30	60	No	No	5
18	30	60	Yes	Yes	15
19	15	45	No	No	5
20	15	60	No	No	5
21	15	60	Yes	Yes	15
22	0	45	No	No	5
23	0	60	No	No	5
24	0	60	Yes	Yes	15

Table 4. Wind loading series III: incrementally increase wind speed (both specimens)

Run	Angle (deg)	Maximum Wind Speed	Longitudinal Turbulence	Lateral Turbulence	Duration (minutes)
25	0	70	No	No	5
26	90	70	No	No	5
27	90	80	No	No	5
28	0	80	No	No	5

29	0	90	No	No	5
30	90	90	No	No	5

Table 5. Wind loading series IV: investigate the response under the maximum speed (Generic specimen)

Run	Angle (deg)	Maximum Wind Speed	Longitudinal Turbulence	Lateral Turbulence	Duration (minutes)
31	270	100	No	No	5
32	0	100	No	No	5
33	0	110	No	No	5

Table 6. Wind loading series IV: investigate the response under the maximum speed (AAF specimen)

Run	Angle (deg)	Maximum Wind Speed	Longitudinal Turbulence	Lateral Turbulence	Duration (minutes)
31	90	100	No	No	5
32	90	100	No	No	5
33	90	100	No	Yes	5
34	90~0	100	No	Yes	5
35	90	100	No	Yes	5
36	90	100	No	Yes	5
37	90	100	No	Yes	5
38	90	100	No	Yes	5
39	270	100	No	Yes	5
40	255	100	No	Yes	5

6. Observations during the Experiment

6.1. Generic Specimen

The generic specimen did not show any significant damage until Run 27 (80 mph). During Run 27, one 2X1 screen attachment failed and caused large movement of the attached screen as shown in Figure 16. The failed member was inspected after Run 27, which showed that the failure was due to the pullout of inner screws (Figure 17). The attachment had permanent distortion but it was still attached to the adjacent structural member.

Run 28, the same maximum wind speed but applied at the wind angle of 0 degree, showed very similar behavior. Two 2X1 screen attachments at the upper center part of the windward wall failed in a similar way. When the maximum wind speed increased to 90 mph at Run 29, one 2X1 member further detached from the structure as shown in Figure 18. This particular stayed attached at one corner without causing failure of the main structural member.

The next load case was Run 30, with the maximum wind speed of 90 mph applied at the wind angle of 90 degrees. One 2X1 member detached from the structure as shown in Figure 19. Similar failure occurred to one additional 2X1 member next to the host structure, which fluttered while staying attached to the structural member. The failed members were visually inspected after the Run 30. As shown in Figure 20, unlike the cases so far, failure of the 2X1 member caused failure of structural members. The failed structural members were the vertical post attached to the host structure and the member below the eave.

Due to the unexpected failure of the screens in both 0 degree wind angle and 90 degree wind angle, we were not able to fully load the generic specimen. The maximum wind speed that the structural members experienced was 80 mph, because at 90 mph screens began to fail. After completing Run 30, these failed screens were re-installed, with the exception of the corner shown in Figure 20 where re-installation was

not possible. It was decided to add additional screws (in between the installed screws) to prevent failure of the screens. The goal was to apply larger forces to structural members without premature failure of the screens.

The wind angle was adjusted to 270 degrees (instead of 90 degrees) in Run 31 to utilize fully intact windward screens on that side. The maximum wind speed was increased to 100 mph. Run 32 also had the maximum wind speed of 100 mph, but applied at 0 degree wind angle. In both tests there were no visible failure of structural members. Only some 2X1 screen attachment continued to fail as shown in Figure 21.

Figure 16. Partial failure of the screen attachment during Run 27 (maximum wind speed = 80 mph)

Figure 17. Partial failure of the screen attachment due to the pullout of screws (after Run 27)

Figure 18. Failure of the screen attachment during Run 29 (maximum wind speed = 90 mph)

Figure 19. Failure of the screen attachment during Run 30 (maximum wind speed = 90 mph)

Figure 20. Failure of the structural members after Run 30

Figure 21. Failure of the screen attachment during Run 32 (maximum wind speed = 100 mph)

6.2. AAF Specimen

Overall, the AAF specimen responded similar to the generic specimen. No significant damage was observed until 80 mph, when some screen attachments began to fail partially as shown in Figure 22. At 90 mph 0 degree wind angle (Run 29), the second screen panel from the far end failed as shown in Figure 23. At 90 mph 90 degree wind angle (Run 30), the first screen panel from the far end failed in a similar fashion. Figure 24 compares failed screen attachments between the generic specimen and the AAF specimen after completing the Run 30.

While the generic specimen had to undergo re-screening due to the loss of three (out of four) upper windows as well as change of loading direction in Run 31, the AAF specimen was subjected to 100 mph wind speed immediately after the Run 30. During Run 31, the screen attachment of the second window from the far failed, but the failed member dangled in the corner and fluttered. Therefore, the upper column was continuously subjected to the large force even after the failure of the screen. The upper column was significantly damaged in the process as shown in Figure 25. While investigating the failure, the thickness of this column was compared between the generic specimen and the AAF specimen. For the generic specimen, the thickness of the flat part and the grooved part were 0.045 inch and 0.061 inch. For the AAF specimen, the thickness of the flat part and the grooved part were 0.042 inch (–6%) and 0.059 inch (–3%). It is possible that slightly less thickness of the AAF member contributed to the failure, but given the small difference the fluttering of the dangled screen attachment was likely cause of the failure of this column.

We decided to further investigate why the column has failed. The windward wall (at 90 degrees wind angle) was retrofitted by replacing the two interior posts with intact members from the generic specimen. All failed screens were repaired with new screens. Additional screws were added to the screen attachments to prevent the failure of the screen attachment, and to fully load the specimen. Run 32 then was conducted, which was identical to Run 31. Turbulence was added at Run 33. Wind angle was changed from 90 degrees to 0 degree in Run 34. The corner screen was cut in Run 35 to introduce unbalanced loading to the column. Extra screws in the screen attachment were removed in Run 36.

Additional screws from the second window attachment were removed in Run 37, so that the attachment would fail similar to what happened in Run 31. Under these conditions, i.e., wind loading from only one of the two sides and failed screen attachment, the column failed again as shown in Figure 26.

While the specimen was retrofitted after Run 31, we visually checked failure at other locations. It appeared that cables lost tensions significantly (but not completely) during the series of runs. We also found out that brackets at the base of the post (windward wall for 0 degree wind angle, third post from the left) had local failure as shown in Figure 27. It was unclear if the failure was from a specific load case, or repeated high moment at the base during the series of runs.

Run 38 was an attempt to investigate the effect of the additionally installed screws to the screen attachments. Extra screws in windward wall of 0 degree wind angle were removed in Run 38. Runs 39 and 40 were attempts to investigate poorly constructed cables. Poorly constructed cables can be pulled out from the ground or the mount during the hurricanes. In these tests tension cables were removed from the specimen. When the wind loading was applied greater moment was applied to the screen-to-host connections and one of these connections failed as shown in Figure 28.

Figure 22. Partial failure of the screen attachment during Run 27 (maximum wind speed = 80 mph)

Figure 23. Failure of the screen attachment during Run 29 (maximum wind speed = 90 mph)

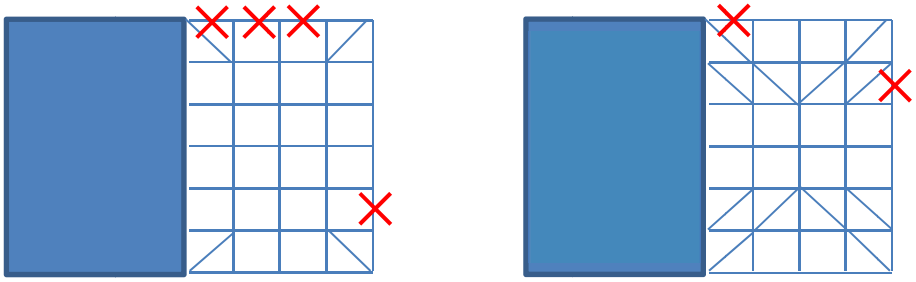

Generic specimen AAF specimen

Figure 24. Comparison of failed screens and/or screen attachments (fully failed ones only) between the generic specimen and the AAF specimen after Run 30 (maximum wind speed = 90 mph)

Figure 25. Failure of structural members after Run 31 (maximum wind speed = 100 mph)

Figure 26. Reproduction of failure of the column in Run 37: unbalanced loading with the failed screen attachment led to the failure of the column

Figure 27. Local failure of brackets at the base of the post (windward wall for 0 degree wind angle, third post from the left)

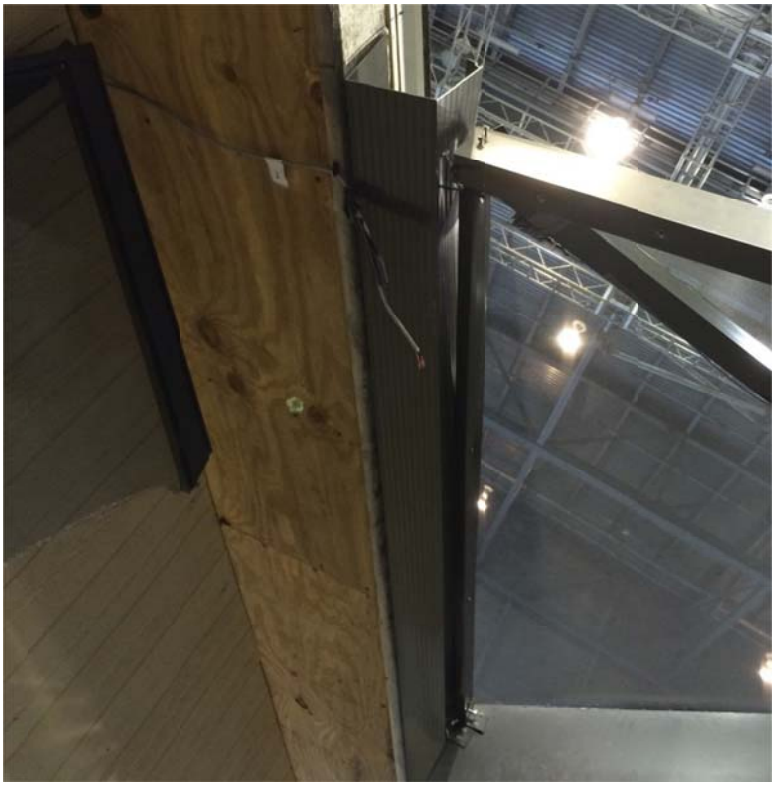

Figure 28. Failure of a screen-to-host connection after Run 39 (removed tension cables, wind angle = 270 degrees, maximum wind speed = 100 mph)

7. Finite Element Analysis and Comparison to Experimental Data

7.1. Material Properties from the Tension Testing

The material used in the screen enclosure was labeled as 6005-T5. Although published properties of this material were available (E = 10,100 ksi, σ_y = 35.0 ksi, σ_u = 38.0 ksi), tensile testing was conducted to measure properties directly from the specimen. Four testing coupons were harvested from a 2X2 member and eight testing coupons were harvested from a 2X6 SMB member. Figure 29 shows the material testing machine and the members after harvesting the coupons.

Material properties were obtained after testing the 12 coupons. The average elastic modulus was 9,300 ksi, which was used in the analysis instead of the published value. The yield stress and the ultimate stress were also lower than the published values. The mean and the standard deviation of the yield stress were 32.3 ksi and 1.2 ksi, resulting in a statistically calculated minimum of 27.8 ksi (vs. 35 ksi specified minimum). The mean and the standard deviation of the ultimate stress were 37.5 ksi and 0.9 ksi, resulting in a statistically calculated minimum of 34.0 ksi (vs. 38 ksi specified minimum).

Figure 29. Material testing machine (left) and 2X2 and 2X6 SMB after harvesting testing coupons (right)

7.2. Calibration of the Finite Element Model

The preliminary finite element model assumed that all boundary conditions allow rotations and that most connections allow rotations (see Figure 1). Two additional modeling assumptions are compared to the baseline model in order to use the most representative finite element model in the further analysis. Figure 30 summarizes the three different modeling assumptions. Pull 01 and Pull 03 cases are used for comparing the models (see Figure 13).

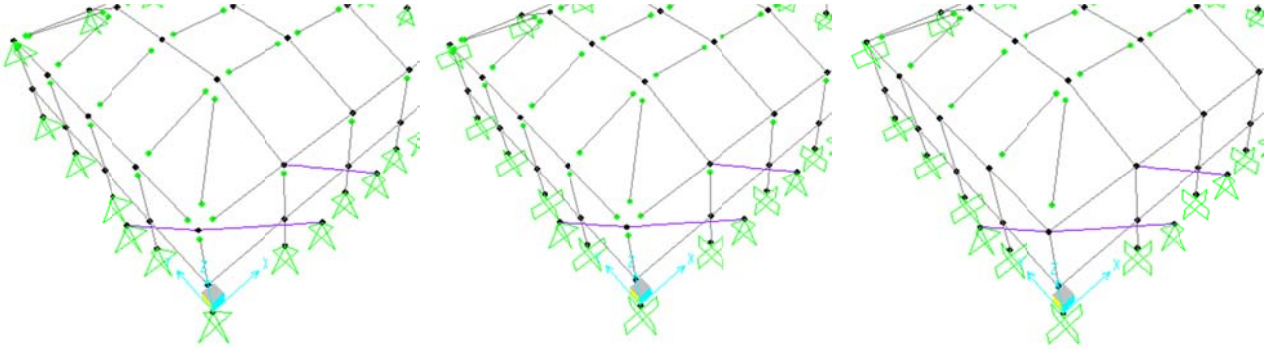

Figure 30. Comparison of three different modeling assumptions. Left (Model A): the baseline model shown in Figure 1, Center (Model B): assume that the boundary conditions prevent rotation, Right (Model C): in addition, frame-end releases are all fixed except in the purlins and corner bracings

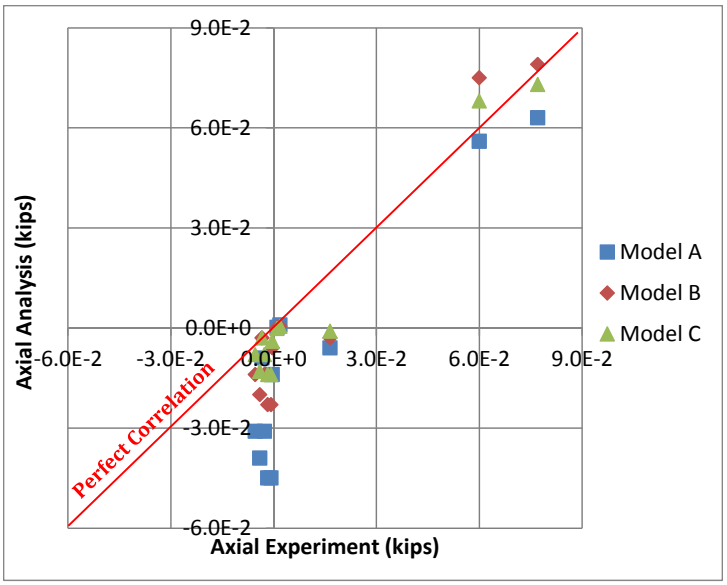

Figure 31. Axial force results for AAF, Pull 01 load case

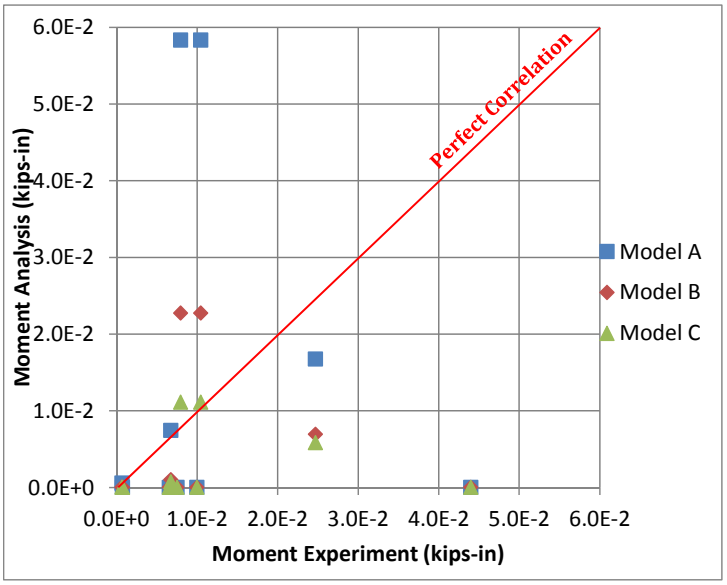

Figure 32. Moment results for Generic, Pull 01 load case

Among various analysis results, two sample results are shown in Figure 31 and Figure 32. Each data point represents forces or moments in one of the sensor locations (see Figure 11, Figure 12). X-coordinate comes from the sensor reading in the experiment. Y-coordinate comes from the forces or moments in the finite element analysis. Therefore, a perfect correlation between the experiment and the analysis will be aligned along Y = X line shown as the red line.

Model C is chosen for further analysis after comparing the performance of the three modeling assumptions. Axial forces overall showed good match between the experiment and the analysis. Moments were less accurate, probably in part due to the small magnitude of the applied force and in part due to the inaccuracy in connection modelling. All finite element models assumed either completed fixed or free connections, whereas the true behavior would be in between these two. Finally, the cable forces had most error between the experiment and the analysis. The analysis could not reproduce the measurement.

7.3. Comparison of the Design Loading and Actual Loading

Before comparing the analysis results and experimental data, we need to understand the relation between the design loading used in the analysis and actual loading applied in the experiment. The design loading is clear because we followed the loading given in the Florida Building Code (see section 4.1). The design loading is for 120 mph Exposure B. The actual loading can only be estimated because it was not measured. We estimated the actual loading using the wind speed profile of the IBHS center (Morrison et al. 2012) and the drag coefficient of 0.7 (Reinhold et al. 1999), which includes the gust effect, drag, and screen reduction factor. In the comparison and further analysis below, 90 mph was chosen as the maximum load case. The reason is because comparison at 100 mph was difficult due to the difference in failed screens between the Generic and the AAF specimen and loss of sensors at this speed.

Figure 33 compares the design loading and the actual loading for the windward wall. At the reference height of 33 ft, actual loading is greater than the ASD loading but smaller than the LRFD loading. However, below 11 ft where the screen enclosure is located, the design loading is always greater than the actual loading. The trend is similar to the leeward wall, but the design loading is lower than the windward case. To compare the total loading approximately, base shear and base moment were also computed assuming freestanding walls. Figure 34 summarizes the comparison.

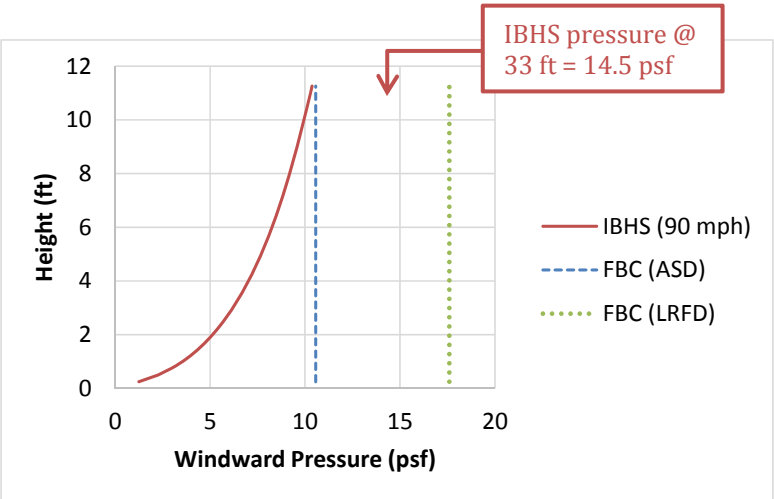

Figure 33. Comparison of the design loading and the actual loading

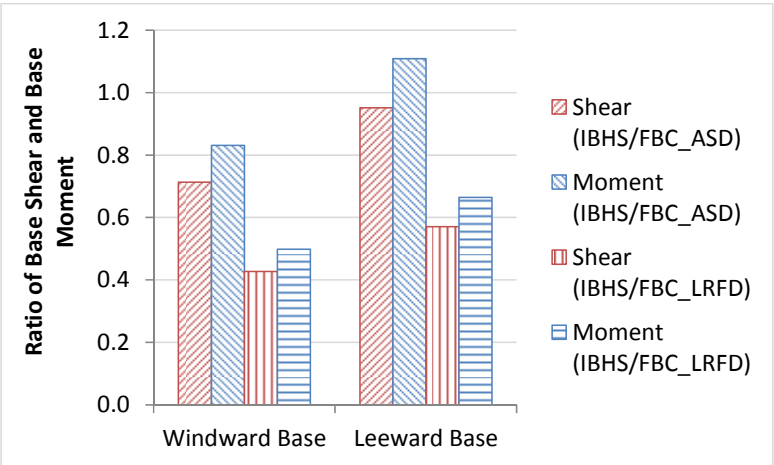

Figure 34. Ratio of the actual to design base shear and base moment

7.4. Comparison of the Analysis and Experiment

As shown in Figure 33 and Figure 34, the actual loading applied in the experiment is lower than the design loading used in the analysis. Therefore, data (force or moment) from certain sensor should also be lower than the corresponding result from the analysis. If the experimental data is higher than the analysis result, possible causes include localized effect of the wind gust, and discrepancy between the finite element model and the physical specimen. In this project, we investigated those data points in detail (i.e., experiment > analysis) focusing on implications on the current design code, but we did not investigate the exact cause. Further research is necessary to identify the cause.

Unlike the pull tests presented earlier, data from wind tests fluctuate due to the fluctuations of the wind. Figure 35 shows sample time-series from Run 28, for the sensor A-6 of the Generic specimen. The original time series was 300 seconds but only the first 30 seconds is shown here. The change in force was measured with respect to the initial condition, after the gravity and the cable tensions were applied. This particular member was subjected to the compression when the wind loading was applied. The force fluctuated because of the fluctuations of the wind. In order to compare this type of data with the static finite element analysis, the mean and the maximum of the time-series were used. In the example shown in Figure 35, the mean = –0.466 kips and the maximum (compressive force) = –0.579 kips.

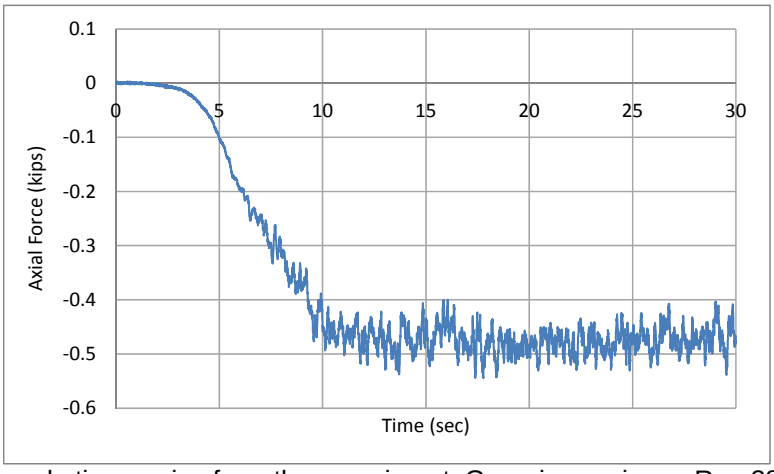

Figure 35. Sample time-series from the experiment: Generic specimen, Run 28, sensor A-6

Experimental data from the Generic specimen is first compared to the analysis result. Maximum measurement from each sensor was compared to the corresponding analysis result as shown in Figure 36. Similar figures for other wind angles and moments can be found in the Appendix (section 11.3). For the square markers, experimental data from 80 mph test were used. For the diamond markers, experimental data from 90 mph test were used. For both markers, analysis results using FBC ASD loading were used. All sensor data were used for 80 mph case, but sensors 7, 13, 15, and 17 failed during the 90 mph test. In this figure, we can see that tensile forces from the experiment are smaller than those from the analysis, except for tensile forces of small magnitude. Therefore, if the structure can sustain the high tensile forces shown earlier in Figure 2, no additional members raise any concern. On the other hand, compressive forces from the experiment are larger than those from the analysis for some members. What this implies is that the current design loading with conventional finite element analysis may not catch potential failure of these members. These sensor locations are marked for further investigation.

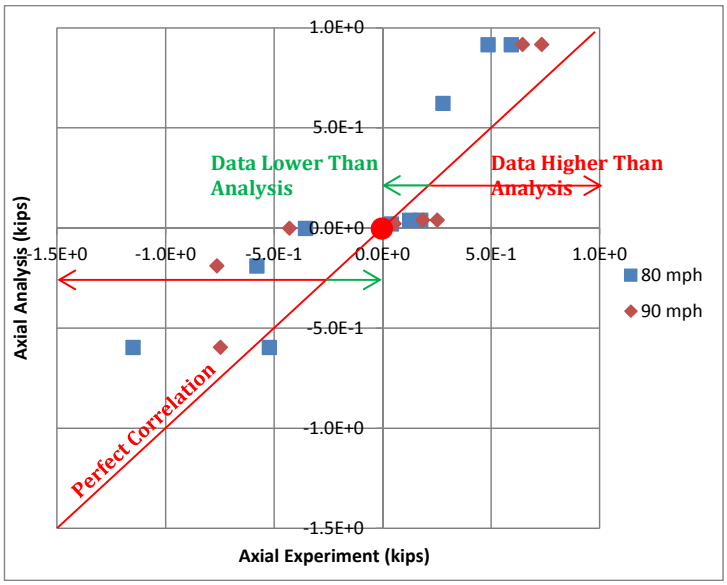

Figure 36. Comparison of the data from the experiment and results from the analysis: Generic specimen, 0 degree wind angle, axial forces

Figure 37 graphically shows the marked sensor locations. Corner bracings, the center post on the windward wall (for 90 degrees wind angle), and members next to the cables showed high experimental measurement. These locations experience higher localized forces than what's predicted by the finite element analysis. For these members, actual to allowable stress ratios were computed for members in compression or bending, using both the maximum measurement and average measurement. For the members in tension, tensile forces were obtained. The results are summarized in Figure 38. All sensors used the data from 90 mph tests except the sensors failed at that speed, for which the data from 80 mph tests were used. The only member that exceeded the allowable stress is the corner bracing with the sensor A-1. The member did not buckle probably because the actual connections at the ends provide shorter length for buckling, compared to the length used for the allowable stress calculation.

When we compare high moment locations (M-17, M-18) with the location that lost the screen attachment (see Figure 24), we can hypothesize that high moment contributed to the failure of the screen attachment. We can also hypothesize that overall higher moments in the Generic specimen led to greater loss of screen attachments compared to the AAF specimen. With the available data, it is not possible to prove or disprove these points, but these can be further investigated in the future study.

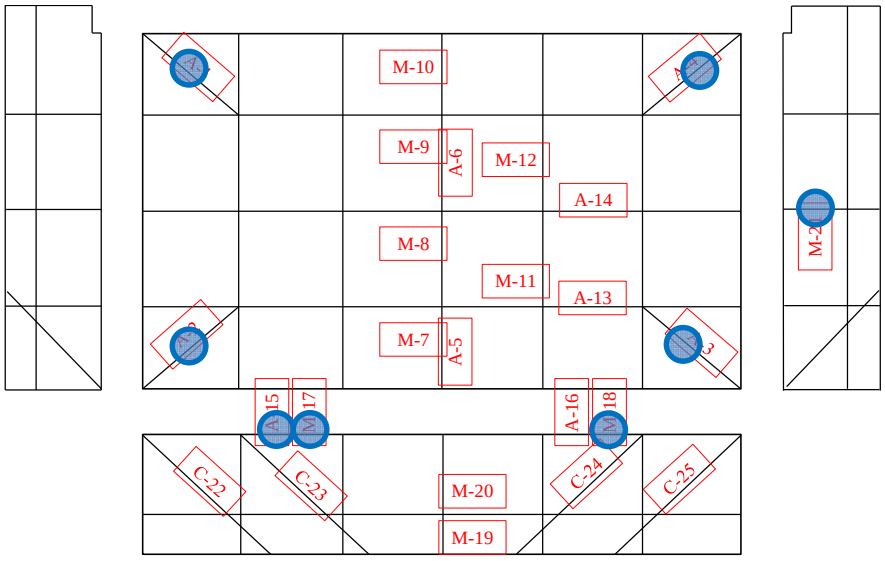

Figure 37. Sensor locations that showed notable forces and moments: Generic specimen

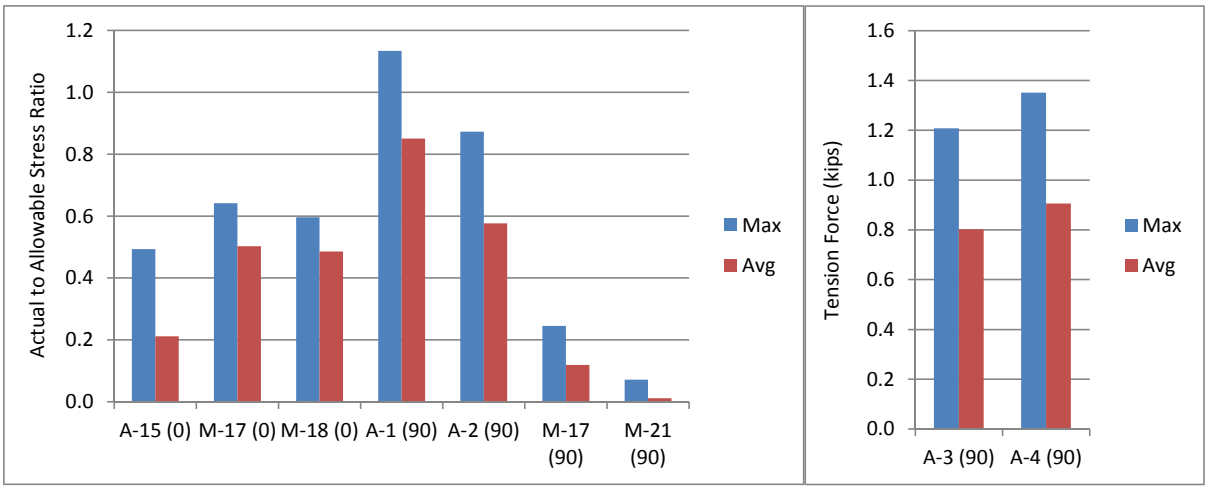

Figure 38. Actual to allowable stress ratio (left) and tension (right) of selected members: Generic specimen

Similar data analysis was conducted for the AAF specimen as shown in Figure 39. Additional figures can be found in the Appendix (section 11.3). All sensors were used except the sensors 3, 12, and 19 due to the poor quality of data. Sensors with notable forces and moments were marked, which are summarized graphically in Figure 40. Similar to the Generic specimen, the posts on the windward wall (for 90 degrees wind angle) and the roof corners showed high forces and moments. The center roof beam also showed high forces and moments.

Figure 41 shows further analysis of these notable locations. All sensors used the data from 90 mph tests. M-18 shows the moment of the vertical post that failed during the 100 mph test. Even at 90 mph, the maximum actual to allowable stress ratio exceeded 1.0. Other sensors also showed large values, but not to the extend to fail the members.

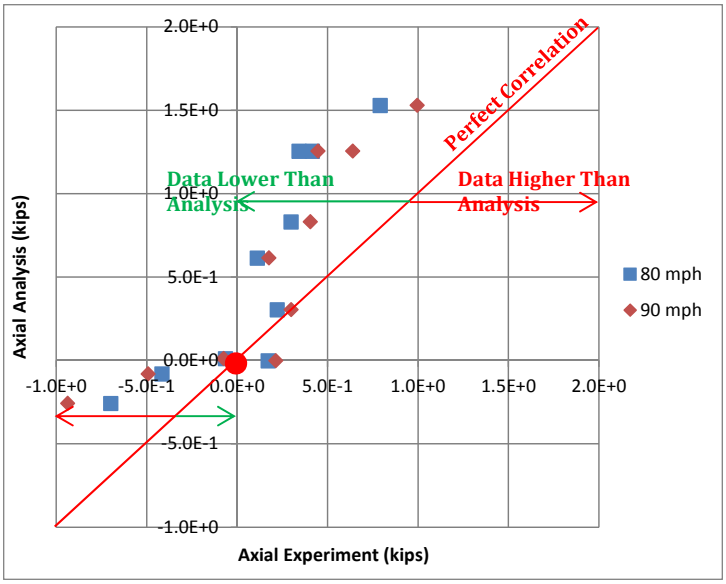

Figure 39. Comparison of the data from the experiment and results from the analysis: AAF specimen, 0 degree wind angle, axial forces

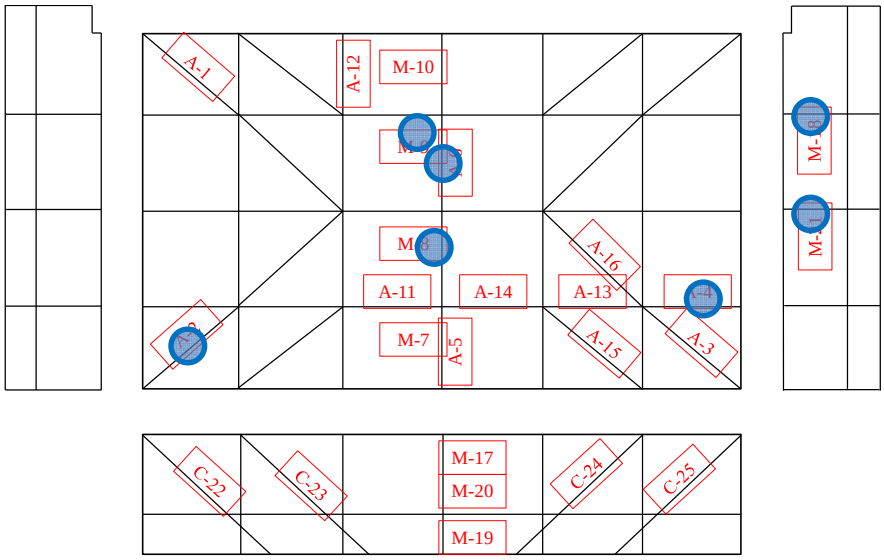

Figure 40. Sensor locations that showed notable forces and moments: AAF specimen

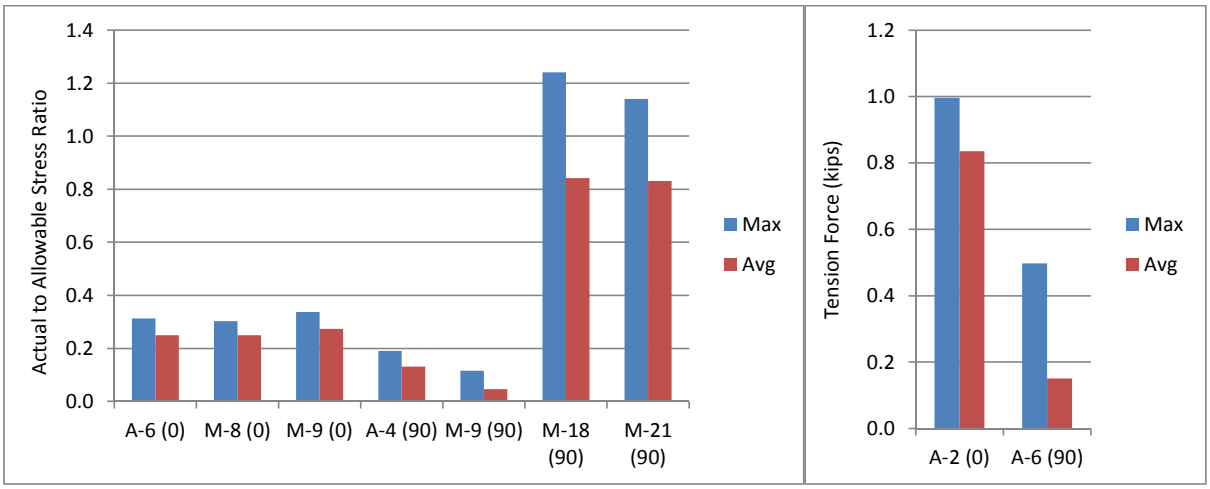

Figure 41. Actual to allowable stress ratio (left) and tension (right) of selected members: AAF specimen

8. Implications to the Code

The wind loading applied during the full-scale tests did not exceed the design loading. In principle, no members should have failed. However, failures occurred at non-structural and structural members. Relevant sections of the code may be revised to reflect the observations. Specifically:

- Screens began to fail at 80 mph.
- Some 2X1 screen attachments failed at 90 to 100 mph. Some of the failed screen attachment fluttered while attached to the structural member, and led to the failure of the structural member.
- One vertical post failed due to the unbalanced loading. One side of the failed post had the screen (and therefore wind loading) whereas the other side did not have the screen.

The failure of screen attachments and unbalanced loading have direct implications on the rule on removing the screen (Rule 61G20-1.002). If some screens are cut but not others, unbalanced loading may accelerate the failure of the post. Code changes should be considered to either require removal of all screens above the chair rail, or, devise a more secure fastening of screen attachments to prevent partial failure and unbalanced loading.

The tested specimens received very thorough inspection and quality control. However, it is well known that the real-world plan review and inspection may not reach such a level, and therefore, likely experience much more severe failure due to the hurricane. The code requirement on this issue would greatly reduce potential failure of screen enclosures due to the hurricane.

Finally, the tensile ultimate strength and tensile yield strength of the aluminum extrusions, based on the testing of coupons harvested from the specimens, were lower than the specified values. To ensure that the aluminum meets or exceeds the specified performance levels, the building code should require that material certification be submitted to the building official.

9. Reference / Project Material

- Aluminum Association of Florida (AAF) (2010), 2010 AAF Guide to Aluminum Construction in High Wind Areas. Available at http://www.aaof.org/resources/aaf-design-guide/aaf-guide-to-aluminum-construction-in-high-wind-areas-non-members/.
- Computers and Structures, Inc. (CSI) (2009), CSI Analysis Reference Manual for SAP2000, Computers and Structures, Inc.
- Florida Building Code (FBC) (2010), The 2010 Florida Building Code: Building

- Hoffmann, K. (1986), Applying the Wheatstone Bridge Circuit, HBM S1569-1.1 en, HBM, Darmstadt, Germany
- Lewis, J., Jung, S., Mtenga, P. (2013), Performance of screen enclosures under repeated loading cycles, ASCE Journal of Performance of Constructed Facilities, v 27, p 415-423
- Morrison, M. J., Brown, T. M., Liu, Z. (2012), Comparison of field and full-scale laboratory peak pressures at the IBHS research center, Advances in Hurricane Engineering, p 1109-1124
- Reinhold, T. A., Belcher, J., Miller, D., Everley, C. (1999), Wind Loads on Screen Enclosures, Unpublished Manuscript
- Schellhammer, M., Jung, S. (2012), Assessment of aluminum screen enclosure connections subjected to strong winds, Engineering Structures, v 43, p 78-87

10. Acknowledgement

This research has been possible thanks to the contributions from many people. This report contains work of those who also participated in the research.

Michael Driscoll provided the Screen Enclosure Structural Calculator and most of the photos in this report. David Miller ran this calculator, provided drawings, and answered technical questions on screen enclosure analysis. He also independently ran finite element analyses, which were used to verify the finite element analysis used in this report. Steven Sincere and Randy Kissell served as technical advisors for aluminum behavior and screen enclosure analysis. The fabrication and assembly of screen enclosure specimens were done by a group of people from the screen enclosure industry. Preparation of strain gauges and data collection were done by Tim Reinhold and Murray Morrison. Gholamreza Amirinia assisted processing of experimental data.

11. Appendices

11.1. Appendix A – Letter from the Aluminum Association of Florida

JDB CODE SERVICES, INC.

Date: September 20, 2013

Florida Building Commission
C/O Mo Madani, DBPR
1940 North Monroe Street
Tallahassee, FL 32399

Subject: Aluminum Association of Florida (AAF) Request for Funding for Full Scale Wind Testing of Aluminum Screen Enclosures

Dear Florida Building Commission:

Please consider this a request for funding for an important research project related to the wind resistance of screen enclosures as defined by the Florida Building Code. During the August meetings at Fort Lauderdale the Florida Building Commission (Commission) adopted a definition for the term "research" as follows:

> "An important and necessary endeavor that aimed at studying specific code related issue(s)/topics for the purpose of providing solutions to a specific problem or future code change(s) directed at improving the implementation and enforcement of the FBC. The issue to be researched must be fully understood (i.e. with clear purpose and goals); clearly defined with specific scope of work/approach; and within budget."

This is to provide data on the research approach for the requested project funding and how the outcomes will be used to improve the Florida Building Code (FBC). The Aluminum Association of Florida requests up to $50,000.00 for full scale testing of the wind resistance of screen enclosures.

Purpose of the Project. The purpose of the project is to evaluate current methods for designing and constructing screen enclosures as defined by the Florida Building Code. Past storms identified problems with engineered screen enclosures in high wind events. The AAF addressed the problems by sponsoring scale model wind tunnel testing at Clemson University and Virginia Polytechnic Institute and State University, hosting a year long series of meetings of contractors and engineers involved in the design of such structures, performing extensive

41 Oak Village Blvd. ● Homosassa ● Florida ● 34446 ● 352-450-2631 ● Fax 813-925-4152 ● joe@jdbcodeservices.com

engineering analysis, developing the Guide to Aluminum Construction in High Wind Areas (Guide), and proposing the Guide for adoption as a prescriptive standard in the Florida Building Code.

The industry is requesting assistance to continue this important work by testing the efficacy of the Guide and to evaluate a sample of popular engineering currently employed in designing and building a common structure found throughout Florida. The specific goal of the project is to increase knowledge regarding the materials and methods of design and construction of screen enclosures using the adopted Guide and using commonly available engineering. Since span lengths and performance of connections are key and have to be evaluated at full-scale, the project needs to test a specimen large enough to embody these features at full-scale.

Scope of the Project. The research proposal is to erect two full scale screen enclosures attached to a host structure and test them at a predetermined wind speed. The enclosures will be tested separately using a uniform wind that follows an open country mean profile with typical small scale turbulence.

Methodology.

1. Estimated time for the project is seven days.
2. AAF will obtain construction documents for a project which has received a building permit based on a submitted engineered design. The source of the documents, contractor, and engineer involved will remain confidential.
3. The design will be for a 130 mph wind speed for Exposure Category C for a screen enclosure with an insect screen roof a maximum of 24 ft. x 40 ft. by 10 ft. with a mansard style roof .
4. AAF will prepare construction documents for the same configuration and parameters for size, height, wind speed, and exposure in accordance with the Guide.
5. AAF will provide all materials, transportation of materials, skilled technicians for the construction, and supervision of the construction.
6.
7. AAF will provide personnel to conduct post-test evaluations
8. A facility of sufficient size capable of performing full scale tests is necessary.
9. The facility responsibilities are:
    a. Provide a host structure,
    b. Provide a foundation system.
    c. Provide and area outside the testing lab where the enclosures can be built.
    d. Provide a means of transporting the structures to the testing lab.
    e. Capable of generating a uniform wind that follows an open country mean profile with typical small scale turbulence of 125-130 mph..

f. Provide sensors on beams to record deflection.
g. The ability to vary the wind direction.
h. The ability to halt and re-start the wind testing.
i. Provide a safe area for viewing the tests.
j. Provide video records of the tests.
k. Provide clean-up post-test.

10. The cost for the testing facility is not to exceed $16,800.00 per day for two days of testing.
11. Funds are requested to cover construction costs estimated at a maximum of $9,000.00.
12. AAF estimates the value of the materials and labor contribution to the project to be $16,000.00.
13. The data generated by the testing will be used to:
    a. Verify or invalidate current practices.
    b. As indicated by test results, AAF will modify existing provisions of the Guide and submit for adoption into the Florida Building Code.
    c. AAF will explore the use of the data gleaned from the tests to develop provisions for retrofitting existing screen enclosures to improve their ability to withstand high winds.
    d. Advise the Florida Engineering community of the results of the testing.

Thanking you in advance for your consideration in this matter.

Respectfully submitted,

Joseph D. Belcher

Joseph D. Belcher

Cc: David Johns, President AAF
David W. Miller, Chairman, AAF Technical Committee

11.2. Appendix B – AAF Design Plans and Rendering of Structural Model

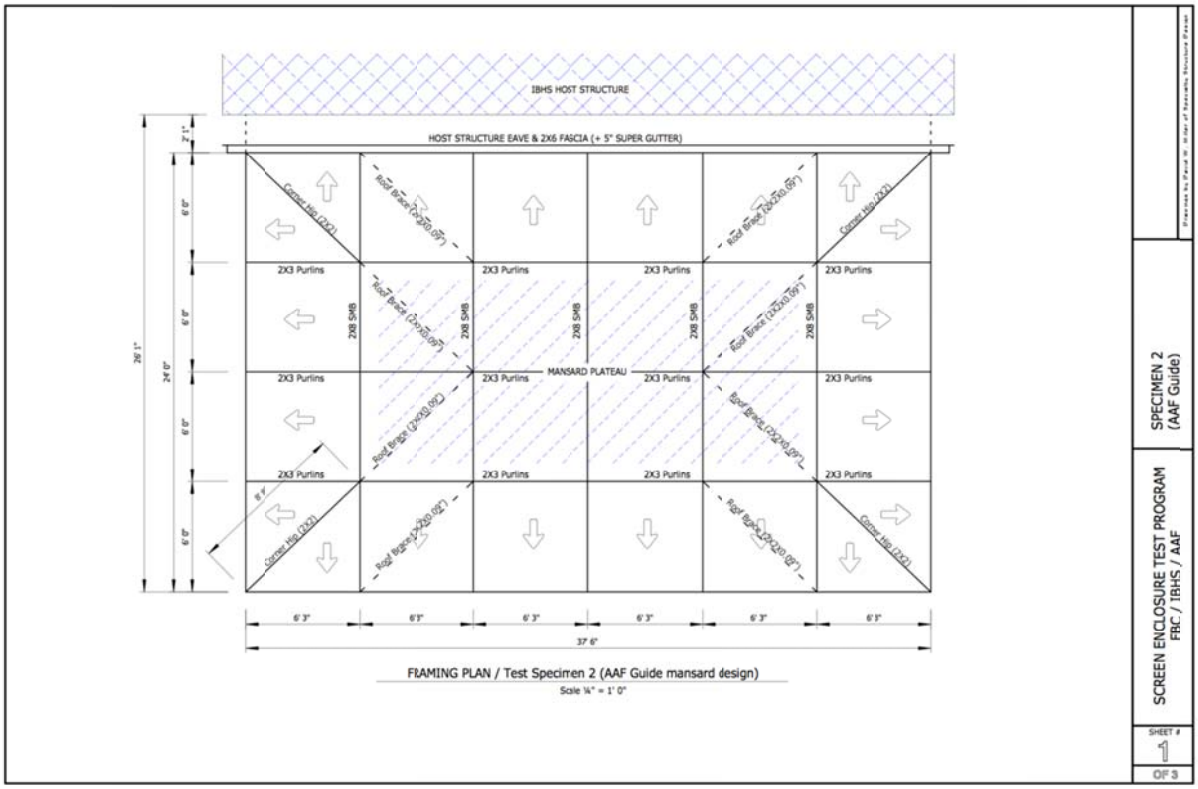

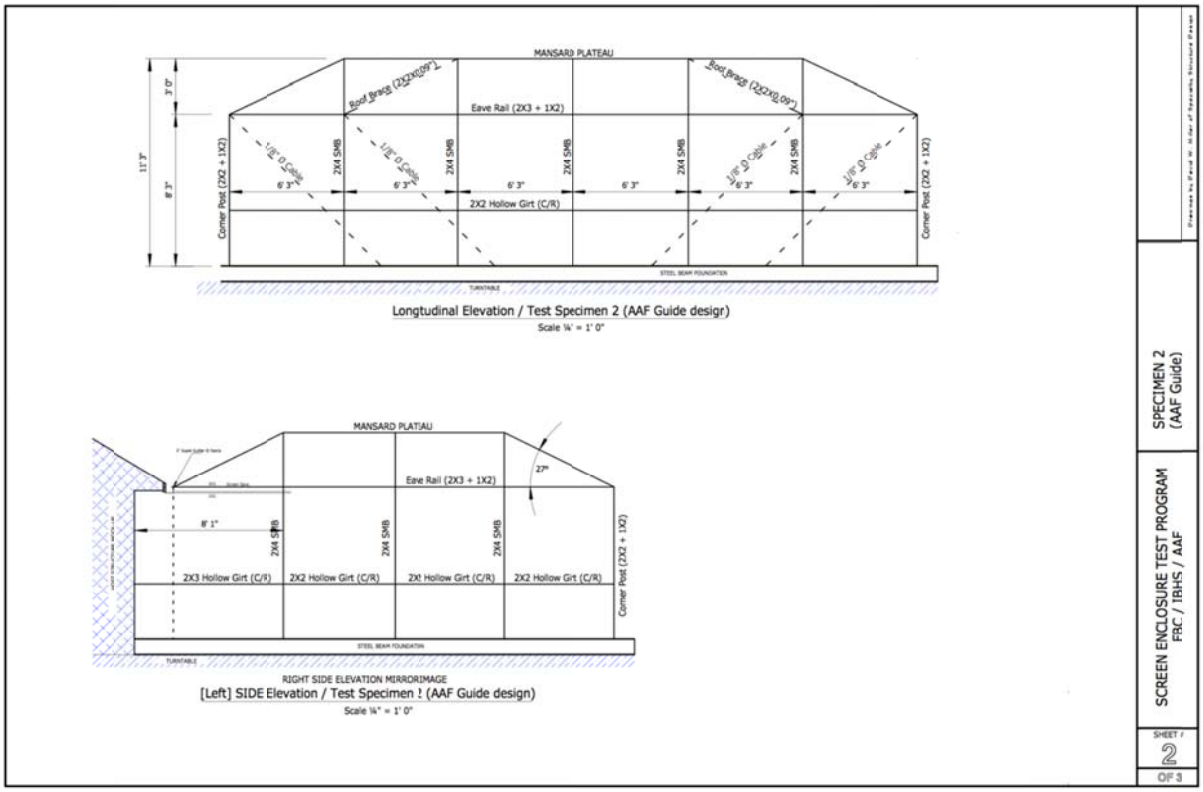

11.3. Appendix C – Comparison of the Experimental Data and the Analysis Results

Experimental data are from 80 mph tests and 90 mph tests. Analysis results are obtained by applying FBC ASD wind loading case explained in section 4.1. The rest of the figures are given in section 7.4 and section **Error! Reference source not found.**.

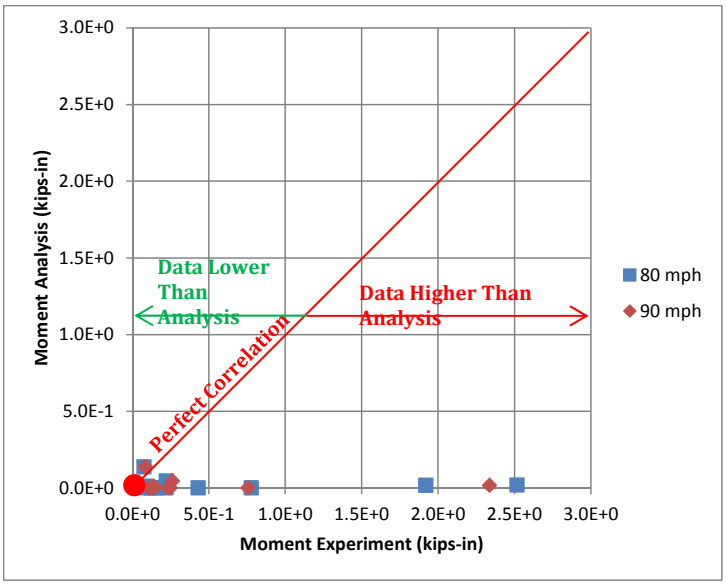

Generic, 0 degree wind angle

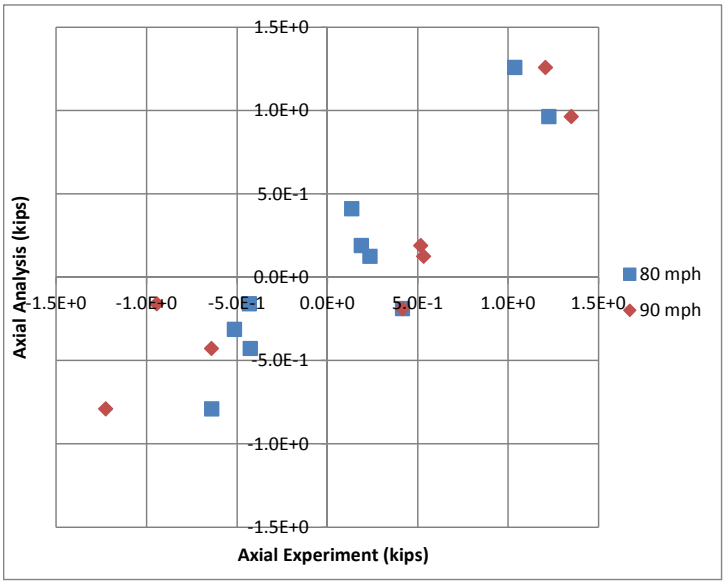

Generic, 90 degrees wind angle

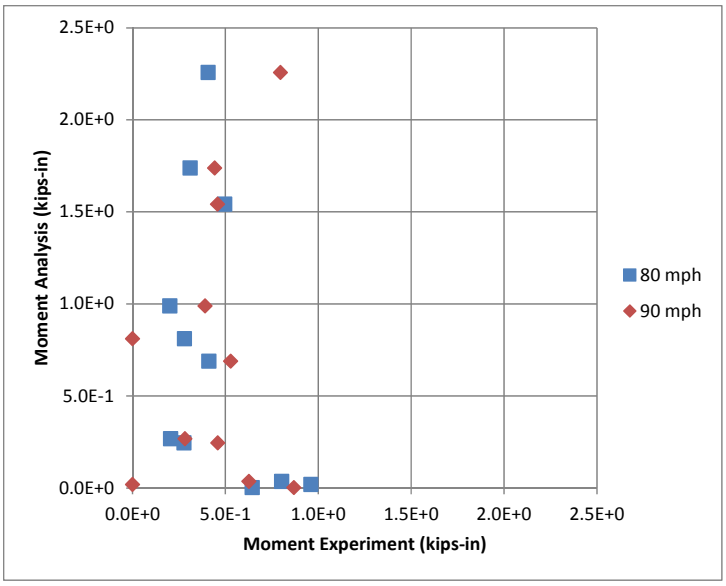

Generic, 90 degrees wind angle

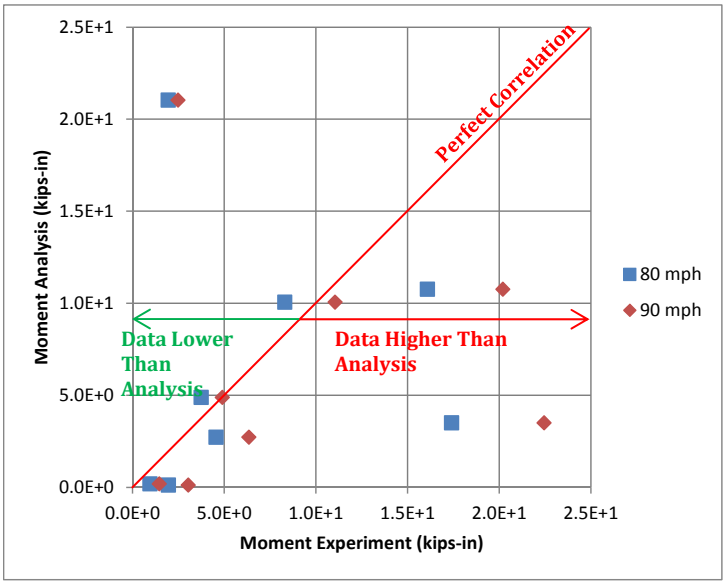

AAF, 0 degree wind angle

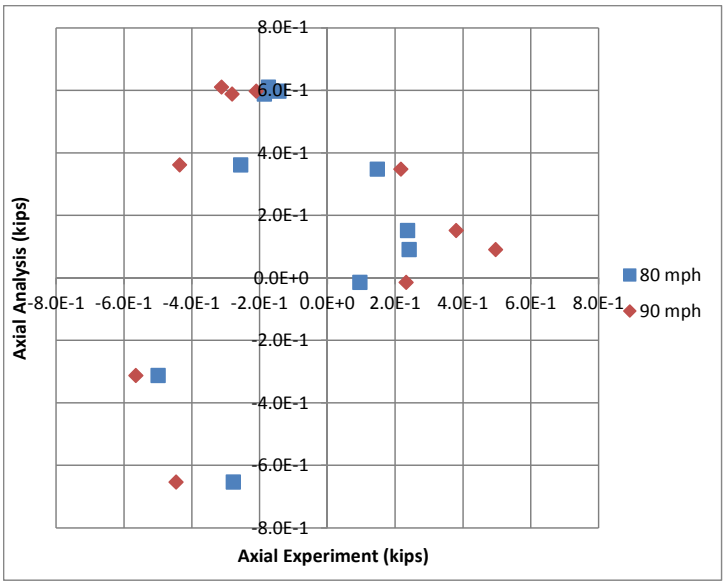

AAF, 90 degrees wind angle

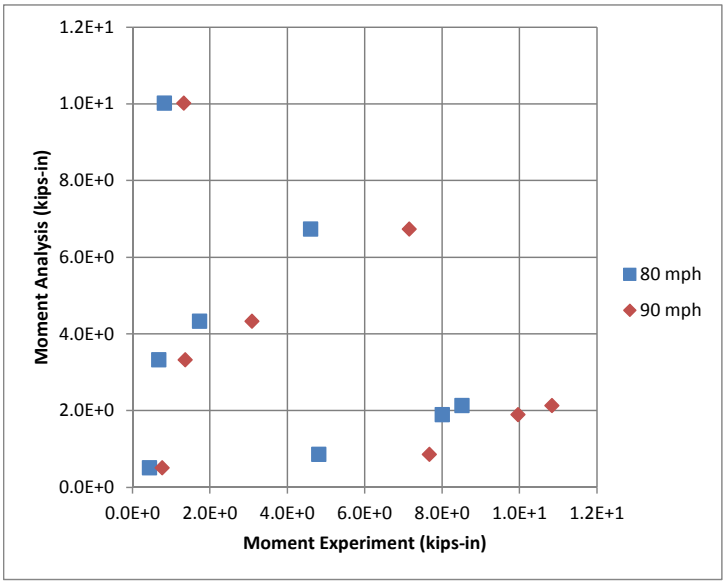

AAF, 90 degrees wind angle